

Supplementary Information

Branched Side Chains Govern Counterion Position and Doping Mechanism in Conjugated Polythiophenes

Elayne M. Thomas,¹ Emily C. Davidson,² Reika Katsumata,² Rachel A. Segalman*^{1,2} Michael L. Chabinyc*¹

¹*Materials Department, University of California, Santa Barbara CA 93106*

²*Department of Chemical Engineering, University of California, Santa Barbara CA 93106*

*Corresponding author's email: mchabinyc@engineering.ucsb.edu, segalman@ucsb.edu

Section 1: Experimental Details

Materials. Regioregular P3EHT was synthesized using a previously reported method ($M_n = 16000$ g/mol).¹ P3HT was purchased from Rieke Metals ($M_n = 58000$ g/mol) and used as received. F₄-TCNQ was purchased from TCI America, and HTFSI was purchased from Acros Organics and used as received. Anhydrous chlorobenzene was purchased from Sigma-Aldrich.

Thin Film Preparation. Thin films were prepared on silicon substrates (300 nm thermal oxide, University Wafer) for atomic force microscopy, and z-cut quartz substrates (University Wafer) for conductivity and UV-Vis measurements. Substrates were sonicated for 10 minutes sequentially in soapy water, DI water, and an IPA/acetone mixture, followed by exposure to UV-ozone (Jelight, Model 18) for 5 minutes. Gold contacts (20 nm) were thermally evaporated on the quartz substrates using a shadow mask. Neat P3EHT (10 mg/ml, chlorobenzene) was spun cast at 1500 rpm to afford 40-nm thick films. Films were annealed at 100 °C for 10 minutes under nitrogen and quenched to 25 °C for 80 minutes.

Vapor Doping. Vapor doping was performed using a sealed vessel, described in a previous publication.² In short, pristine films are attached to the lid of a jar that contains crystals of solid dopant. The jar is closed and heated for a set of exposure times on a hot plate. The HTFSI-doping vessel was heated at 40 °C and the F₄-TCNQ-doping vessel was heated at 210 °C. Exposures were done incrementally in order to capture several doping levels of the films.

X-ray Characterization. X-ray scattering was conducted on beamline 7.3.3 at the Advanced Light Source (ALS).³ Silver behenate was used as a calibration for the beam center and sample-to-detector distance. 2D GIWAXS scattering images were collected using a Pilatus 2M area detector at an incidence angle of 0.12° with 5–60 s exposure times. The samples were kept under a helium environment during X-ray exposure to minimize sample degradation and scattering from O₂. The collected data were processed using Nika, a 2D data reduction macro on Igor Pro using established procedures. To correct for the grazing incidence geometry, scattering intensity was integrated along a small sector near the missing wedge to obtain 1D profiles near $q_z = 0$.

Atomic Force Microscopy. Topological images were captured using tapping mode with an NT-MDT custom-built atomic force microscope (controller model NTEGRA P9) under ambient conditions. Bruker OTESPA-R3 probes (0.01–0.02 Ω-cm Si, $f_0 = 300$ kHz) were used to complete these measurements. The scan size of each image was 2 μm x 2 μm.

UV-visible spectroscopy. UV-visible measurements were taken using an Agilent Cary 60 UV-Vis Spectrophotometer. Spectra were taken on 0.5 mm-thick quartz substrates.

FTIR spectroscopy. FTIR spectroscopy was performed in a nitrogen atmosphere using a Nicolet Magna 850 FTIR Spectrometer with an InSb detector. Samples were spincast on KBr salt plates (13 x 2 mm, PIKE Technologies) using the same conditions as for other characterization techniques.

Electrical Characterization. All electrical measurements were performed under a nitrogen environment inside a glovebox. Electrical conductivity was measured using a Keithley 6485 picoammeter. Measurements were taken in the in-plane direction using the TLM method to eliminate contact resistance for samples with low conductivity.

Section 2: Analysis of Aggregate Absorption

The model developed by Spano *et al.*^{4,5} describes the absorption spectra, A , of P3HT by Equation 1:

$$A = C \sum_{m=0}^{\infty} \left(\frac{e^{-S} S^m}{m!} \right) \left(1 - \frac{W e^{-S}}{2E_p} \sum_{n \neq m} \frac{S^n}{n! (n-m)!} \right)^2 \frac{\exp\left(-\frac{(E - E_{0-0} - mE_p - 0.5WS^m e^{-S})^2}{2\sigma^2}\right)}{\sigma\sqrt{2\pi}} \quad (1)$$

The Huang-Rhys factor, S , is assumed to be unity. The proportionality constant (C), excitonic bandwidth (W), Gaussian width (σ), and the 0-0 intrachain transition (E_{0-0}) are varying parameters in this model. The characteristic C=C phonon stretch is 0.179 eV for P3EHT.

A Matlab code was utilized to perform a least-square fit for the 0–0, 0–1, 0–2, 0–3, and 0–4 transitions as a function of carrier density. A typical fit is shown in **Figure S1**.

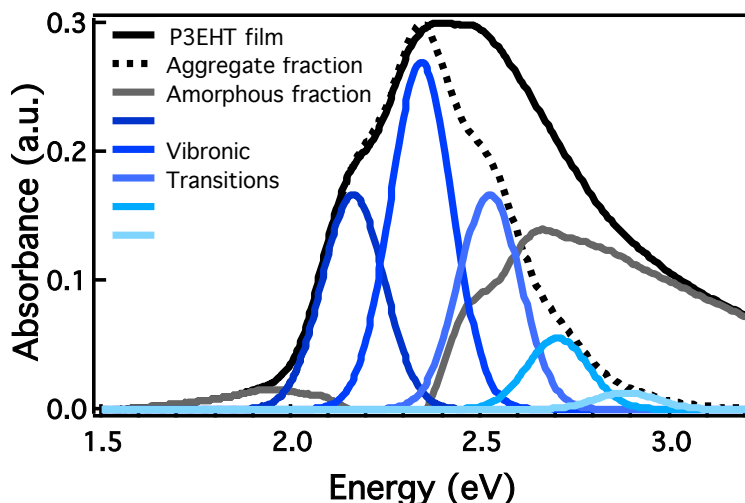


Figure S1: Analysis of P3EHT spectra. The model by Spano *et al.* indicates that about 40% of the P3EHT film is aggregated.

Section 3: Doped solution spectra

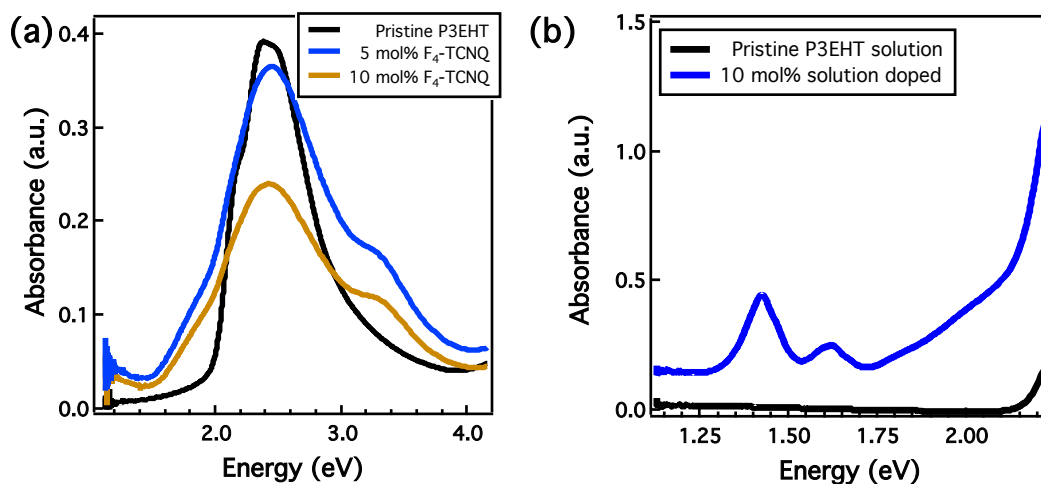


Figure S2: (a) UV-vis spectra of P3EHT films when doped with F₄-TCNQ from solution. Upon film formation from a doped solution, a charge transfer complex forms evidenced by the emergence of similar features as the vapor doped films (Figure 2 in main text) near 3.4 eV, 1.8 eV, and 1.0 eV. (b) Solution spectra of pristine P3EHT (black) and P3EHT with 10 mol% F₄-TCNQ (blue). The familiar peaks corresponding to the anion of F₄-TCNQ appear at 1.4 and 1.6 eV, indicating that the dopant does not complex with the polymer while in solution. Here, data is shown to 2.5 eV since the solvent obscures the spectra at higher energy.

Section 4: FTIR Spectroscopy

The C≡N vibrational stretch of F₄-TCNQ is sensitive to the charge of the molecule. The degree of charge transfer, δ , between F₄-TCNQ and the corresponding acceptor is found using Equation 2:

$$\delta = \frac{2\Delta\nu}{\nu_0} \left[1 - \frac{\nu_1^2}{\nu_0^2} \right]^{-1} \quad (2)$$

where ν_0 corresponds to the neutral value of the C≡N stretch (2227 cm⁻¹), ν_1 corresponds to the frequency of the C≡N stretch for the radical anion (2194 cm⁻¹ corresponding to integer charge transfer (ICT)), and $\Delta\nu$ is the difference between the observed stretch and the neutral C≡N stretch.^{6,7}

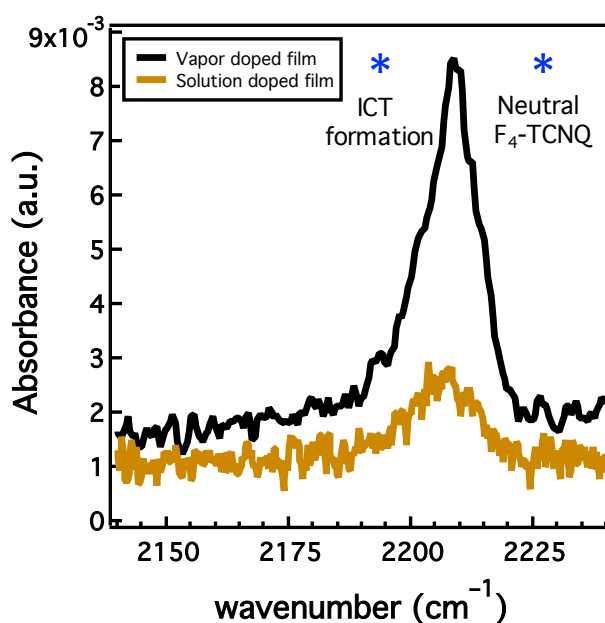


Figure S3: FTIR of heavily-doped P3EHT films from vapor infiltration (black) and from solution casting (orange). The peak corresponding to the C≡N vibrational stretch occurs at 2209 cm⁻¹ for the vapor doped film and 2206 cm⁻¹ for the solution doped film, corresponding to a degree of charge transfer of 0.6. A value of 1 is expected for ICT, such as between P3HT and F₄-TCNQ.

Section 5: P3HT acid doping

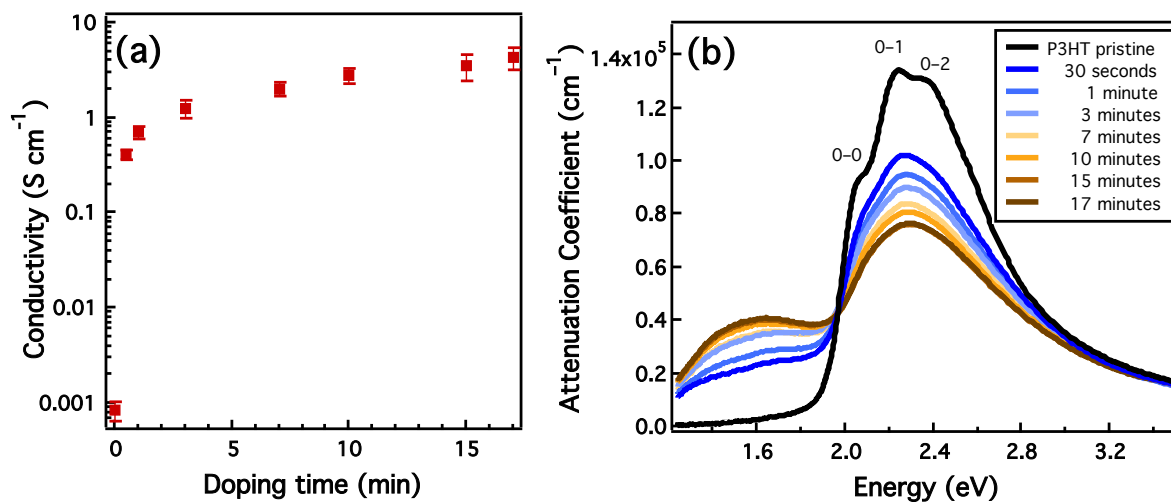


Figure S4: Electrical conductivity (a) and absorption spectra (b) of a film of P3HT with exposure to HTFSI. The resulting electrical conductivity of P3HT is higher than for P3EHT when using the same dopant, potentially due to the differences in intrachain order between the two polymers.⁸ Error bars represent one standard deviation from the average value, taken from triplicate measurements.

Section 6: 2D GIWAXS images of doped P3EHT films

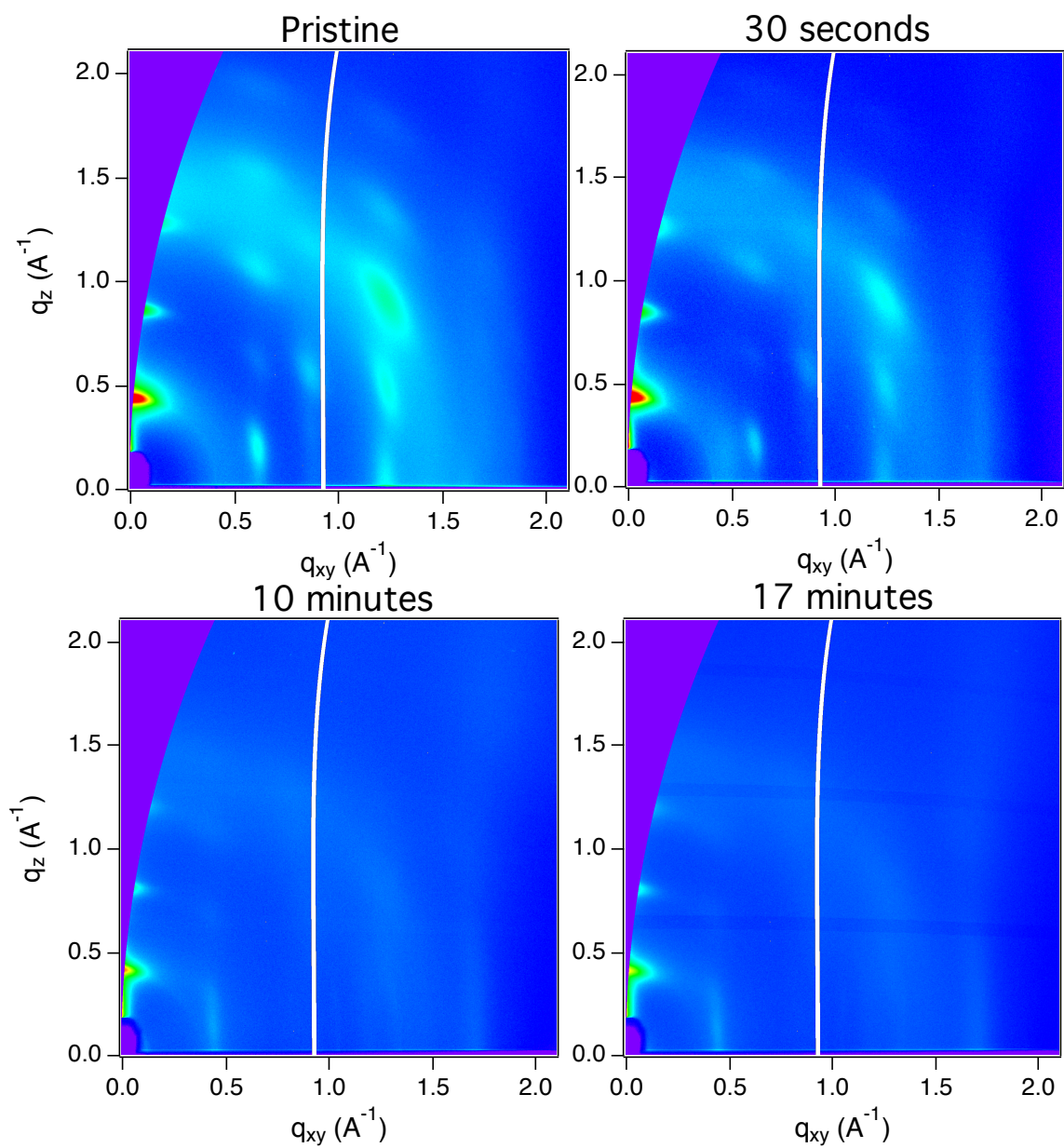


Figure S5: 2D images of P3EHT when exposed to HTFSI. Long exposure times leads to a modified crystal structure and loss of higher order peaks, seen clearly in the 10 minute and 17 minute images.

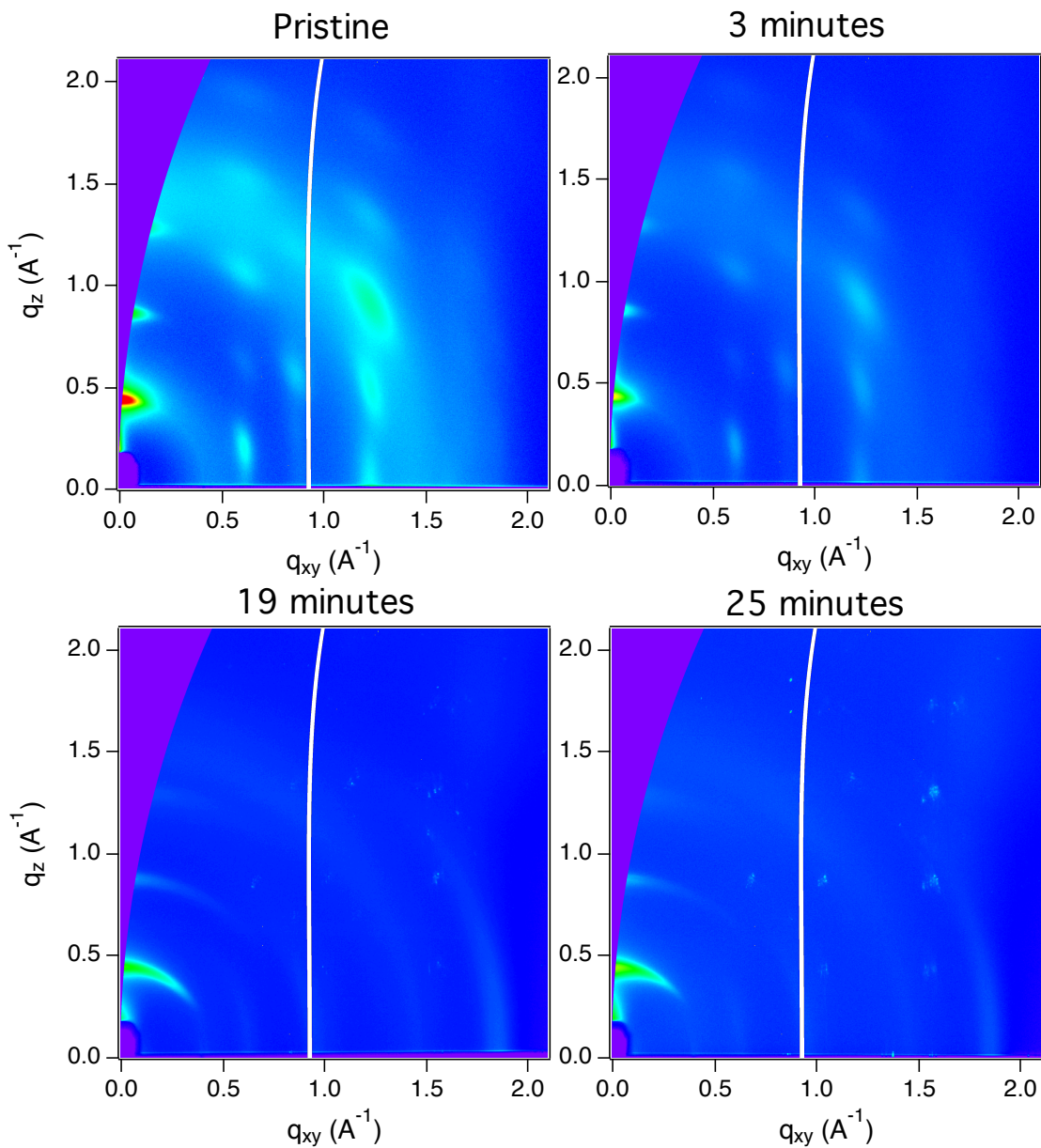


Figure S6: 2D images of P3EHT when exposed to F_4 -TCNQ. Broadening of the peaks along with new features with increasing exposure times is indicative of disorder and a modified crystal structure induced upon infiltration of the dopant. Sharp features seen in the 25 minute image may correspond to F_4 -TCNQ at the surface.

Section 7: Atomic Force Microscopy

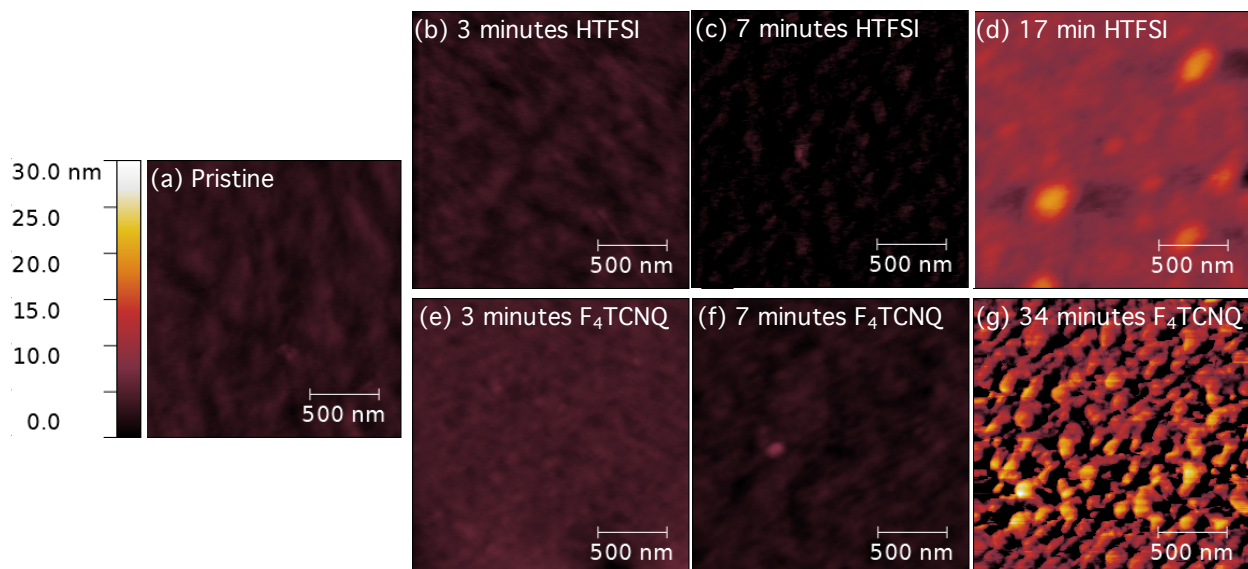


Figure S7: AFM height images of thin films of P3EHT in its pristine form (a) and when exposed to HTFSI and F₄-TCNQ vapor (b-g). Doping with the HTFSI for 3 minutes (b) and 7 minutes (c) introduces little change to the microstructure. Exposure times greater than 17 minutes (d) result in large droplets on the film surface, indicating that the vapor no longer infiltrates the film. A similar effect occurs for F₄-TCNQ vapor after 3 minutes (e) and 19 minutes (f) of exposure time, followed by eventual F₄-TCNQ crystals aggregating at the film surface after 34 minutes (g). All images have the same color map scale bar.

References

- (1) Ho, V.; Boudouris, B. W.; Segalman, R. A. Tuning Polythiophene Crystallization through Systematic Side Chain Functionalization. *Macromolecules* **2010**, *43* (19), 7895–7899.
- (2) Patel, S. N.; Glaudell, A. M.; Kiefer, D.; Chabynyc, M. L. Increasing the Thermoelectric Power Factor of a Semiconducting Polymer by Doping from the Vapor Phase. *ACS Macro Lett.* **2016**, *5*, 268–272.
- (3) Hexemer, A.; Bras, W.; Glossinger, J.; Schaible, E.; Gann, E.; Kirian, R.; MacDowell, A.; Church, M.; Rude, B.; Padmore, H. A SAXS/WAXS/GISAXS Beamline with Multilayer Monochromator. *J. Phys. Conf. Ser.* **2010**, *247*, 012007.
- (4) Clark, J.; Silva, C.; Friend, R. H.; Spano, F. C. Role of Intermolecular Coupling in the Photophysics of Disordered Organic Semiconductors: Aggregate Emission in Regioregular Polythiophene. *Phys. Rev. Lett.* **2007**, *98* (20), 206406:1-4.
- (5) Clark, J.; Chang, J.-F.; Spano, F. C.; Friend, R. H.; Silva, C. Determining Exciton Bandwidth and Film Microstructure in Polythiophene Films Using Linear Absorption Spectroscopy. *Appl. Phys. Lett.* **2009**, *94* (16), 163306.
- (6) Kampar, E.; Neilands, O. Degree of Charge Transfer in Donor–Acceptor Systems of the π – π Type. *Russ. Chem. Rev.* **1986**, *55* (4), 334.

- (7) Chappell, J. S.; Bloch, A. N.; Bryden, W. A.; Maxfield, M.; Poehler, T. O.; Cowan, D. O. Degree of Charge Transfer in Organic Conductors by Infrared Absorption Spectroscopy. *J. Am. Chem. Soc.* **1981**, *103* (9), 2442–2443.
- (8) Chew, A. R.; Ghosh, R.; Pakhnyuk, V.; Onorato, J.; Davidson, E. C.; Segalman, R. A.; Luscombe, C. K.; Spano, F. C.; Salleo, A. Unraveling the Effect of Conformational and Electronic Disorder in the Charge Transport Processes of Semiconducting Polymers. *Adv. Funct. Mater.* **2018**, 1804142.